Summary of Ph.D. thesis

The role of enzyme mimetic Mn(III) porphyrins in the redox reactions of biologically active simple inorganic compounds

József Kalmár

Supervisor: *Dr. Gábor Lente*

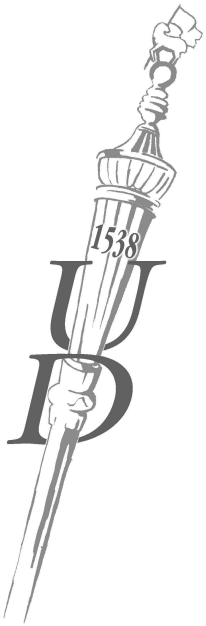

UNIVERSITY OF DEBRECEN
Chemistry Graduate School
Debrecen, 2013

I) INTRODUCTION AND AIMS

Transition metal porphyrin complexes are important and widely used redox catalysts. Their high metal-to-ligand stabilities ensure high turnover numbers and the different side chains attached to the porphyrin core structure help to fine tune the chemical properties of these complexes. As a consequence, industrial synthetic strategies using various polar and nonpolar solvents are often based on metal porphyrin redox catalysts and oxidative wastewater treatment technologies utilizing metal porphyrin catalysts are also currently being developed. Metalloporphyrins play fundamental roles in biological redox reactions as well, as several of the naturally occurring metalloenzymes contain transition metal porphyrin prosthetic groups.

Manganese lacks Fenton chemistry-related toxicity, and provides rich biologically relevant redox chemistry at the metal site. In the past few years, novel synthetic water soluble Mn(III) porphyrins have been developed for therapeutic purposes. Among the most potent *in vivo* superoxide dismutase (SOD) mimics are the ortho and para isomers of Mn(III) meso-tetra-(N-alkylpyridyl), -(N-methoxyalkyl) and -(N-tri(ethyleneglycol))porphyrins. The structures of some selected complexes are given in Scheme 1. Furthermore, the above mentioned cationic and also the anionic $MnTSPP^{3-}$ (Scheme 1) complexes are effective for the removal of peroxynitrite radical *in vivo*. It is well accepted that porphyrins and their metal complexes have affinity for malignant tissues, which forms the basis of the idea of the application of the high relaxivity Mn(III) porphyrins as tumor imaging MRI contrast agents.

Because the biologically important reactions of the Mn(III) porphyrins occur at the metal site and possibly involve the inner sphere coordination of the reactant to the metal center, we found it important to determine the water exchange rates and study the exchange mechanism for representative Mn(III) porphyrins. Four complexes from Scheme 1 were chosen for this study: $MnTEt\text{-}2\text{-}PyP^{5+}$, $MnTnHex\text{-}2\text{-}PyP^{5+}$, $MnTTEG\text{-}2\text{-}PyP^{5+}$ and $MnTSPP^{3-}$.

The high reactivities of Mn(III) porphyrins towards small molecules and the ability to undergo fast axial-ligand substitution during redox cycling are proposed to be key aspects of the *in vivo* and *in vitro* solution-phase chemistry of these complexes. Accordingly, we characterized the biologically relevant redox reaction of a selected SOD mimic Mn(III) porphyrin complex (MnTTEG-2-PyP^{5+} as seen in Scheme 1) with N-hydroxyurea (HU as seen in Scheme 1) *in vitro*. N-hydroxyurea is a hydroxamic acid with a wide variety of antitumor therapeutic applications and has recently been introduced into sickle cell anemia therapy. Patients receiving HU have shown increases in the *in vivo* production of nitric oxide (NO) metabolites. The reason to study the reaction of HU with a Mn(III) porphyrin is that similarly to other hydroxamic acids, HU may act as either a nitric oxide or a nitroxyl (HNO) donor under oxidative conditions, and Mn(III) porphyrins are described to display characteristically different reactivities towards NO donor and towards HNO donor compounds.

The defensive peroxidase enzymes lactoperoxidase myelo-peroxidase and eosinophil peroxidase commonly contain Fe(III) porphyrin (heme) prosthetic groups in their active sites, and among other substrates catalyze the oxidation of SCN^- by H_2O_2 to hypothiocyanite ion ($OSCN^-$ as seen in Scheme 1). Hypothiocyanite ion is a potent bactericide and plays an important role in multiple stages of the non-immune defense system in several physiological locations (e.g., in the mouth and in the airways). Hypothiocyanite ion can be synthesized only in the excess of SCN^- by two-electron oxidation because it can be subsequently oxidized by the same agent (e.g. H_2O_2, HOCl, HOBr) as SCN^-. To elucidate the mechanism of an analogous reaction, we studied the multi-step oxidation of SCN^- with peroxomonosulfate ion (HSO_5^- formulated as Oxone®), where $OSCN^-$ was identified to be an intermediate. The peroxidase mimicking catalytic effect of a selected Mn(III) porphyrin (MnTMe-4-PyP^{5+} as seen in Scheme 1) was also investigated in the $SCN^- + HSO_5^-$ + catalyst reaction system.

The stability and mechanism of hydrolytic decomposition of $OSCN^-$ fundamentally determine its *in vivo* chemical reactivity. It is

known that $OSCN^-$ shows moderate stability at neutral and basic pH and anecdotal reports indicate that its decomposition is faster at low pH and with high concentrations of SCN^-. Considering that thiocyanogen ($(SCN)_2$) yields $OSCN^-$ when it is hydrolyzed at basic pH but does not at neutral pH, one might conclude that the comproportionation of HOSCN and SCN^- to give $(SCN)_2$ is involved in the decomposition mechanism of $OSCN^-$ near neutral pH. Therefore, we investigated the hydrolytic decomposition of both $OSCN^-$ and $(SCN)_2$ in detail at slightly acidic and neutral pH to show that the observed mechanisms are relevant to the stability of $OSCN^-$ at physiological pH.

Abbreviated names of the studied porphyrins:
MnTSPP^{3-}: Mn(III) meso-tetrakis(4-sulfonatophenyl)porphyrin
MnTMe-4-Pyp^{5+}: Mn(III) meso-tetrakis(N-methylpyridinium-4-yl)porphyrin
MnTEt-2-Pyp^{5+}: Mn(III) meso-tetrakis(N-ethylpyridinium-2-yl)porphyrin
MnTnHex-2-Pyp^{5+}: Mn(III) meso-tetrakis(N-hexylpyridinium-2-yl)porphyrin
MnTTEG-2-Pyp^{5+}:
Mn(III) meso-tetrakis(N-tri(ethyleneglycol)pyridinium-2-yl)porphyrin

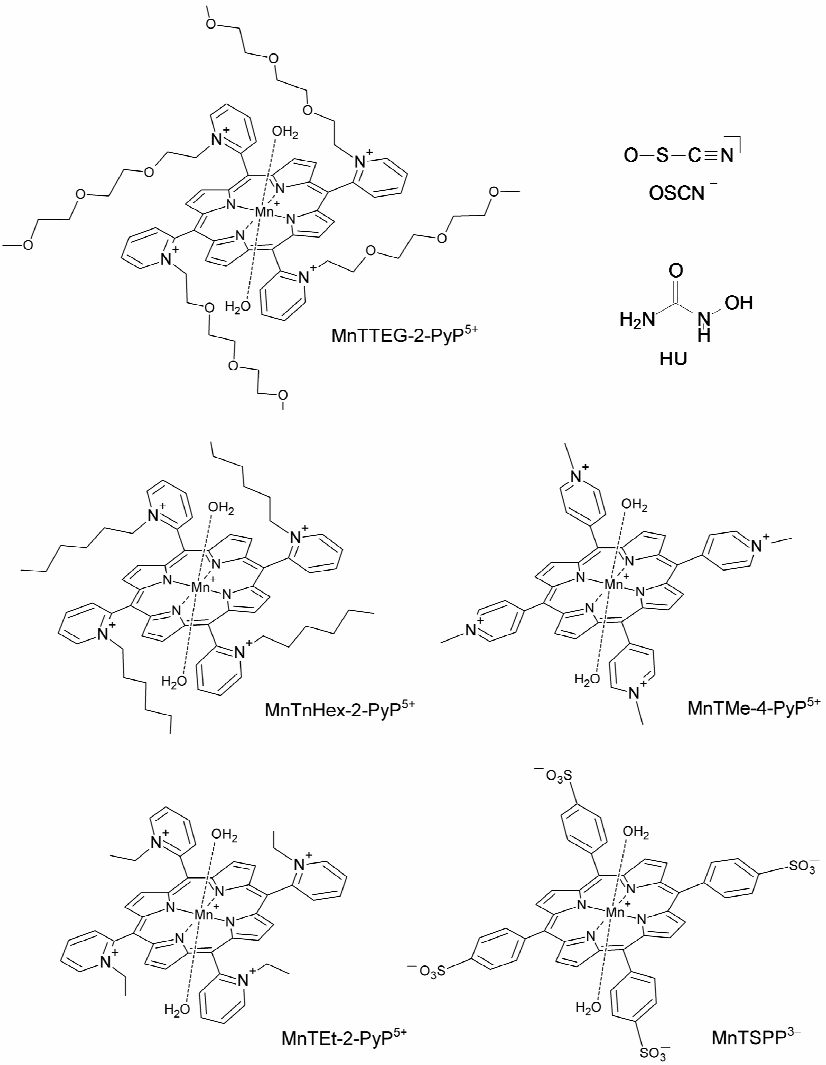

Scheme 1. Structure of the studied compounds.

II) EXPERIMENTAL METHODS

To determine the rates and activation parameters of water exchange of Mn(III) porphyrin complexes **variable-temperature ^{17}O NMR measurements** were carried out in Bruker DRX-400 (9.4 T, 54.2 MHz) or DRX-360 (8.5 T, 48.8 MHz) spectrometers. The measured temperature values were corrected using the "methanol thermometer" method. Longitudinal relaxation rates ($1/T_1$) were obtained by the inversion recovery method and transverse relaxation rates ($1/T_2$) directly from the line widths. The data were analyzed according to Powel and Merbach's previously published procedure (Powel, D. H.; Merbach, A. E. *Magn. Reson. Chem.*, 1994, *32*, 739-745.).

The pK_a values of some selected Mn(III) porphyrin complexes were measured by **UV-vis potentiometric titration**. The spectral change was recorded with a 1.00 cm optical path length spectral probe attached to a Varian Cary 50 scanning spectrophotometer and the pH was measured by a Metrohm 6.0234.110 combined glass electrode attached to a Metrohm 721 NET Titrino unit. The individual spectra of the differently protonated species and the corresponding pK_a values were calculated by the SpecFit/32 software from the recorded pH dependent spectral series.

Hand-mixing kinetic experiments were carried out in a PerkinElmer Lambda 25 scanning UV-vis photometer to study the reaction of HU + Mn(III)TTEG-2-PyP^{5+}. The solutions of HU and Mn(III)TTEG were loaded into a tandem-cuvette and the reaction was started with hand-mixing which usually introduced a ca. 4 s loss (< 1 %) of kinetic data. The kinetics of the reaction of $SCN^- + HSO_5^-$ was studied with **single-mixing stopped-flow UV-vis spectrometry** in an Applied Photophysics DX-17 MV instrument with either a photomultiplier tube (PMT) or a photodiode-array (PDA) installed as the detector. The dead-time of the stopped-flow instrument was determined to be 1.51 ± 0.03 ms by the reaction of 2,6-dichlorophenol-indophenol (DCIP) with ascorbic acid (AA) under

pseudo-first order conditions, allowing the determination of first order rate constants up to $500\ s^{-1}$. To study the kinetics of the decomposition of $(SCN)_2$ or $OSCN^-$ at a given pH **double-mixing stopped-flow UV-vis** measurements were performed. The reagents were generated under either acidic ($(SCN)_2$) or basic ($OSCN^-$) conditions and *in situ* mixed with an appropriate buffer in the second mixing cycle of the stopped-flow instrument to achieve the desired pH. The temperature was maintained within ± 0.1 °C during all stopped-flow measurements with a Julabo F-12 refrigerated/heated circulator.

The products of the reaction of $SCN^- + HSO_5^-$ and the decomposition of $(SCN)_2$ and $OSCN^-$ were studied by **electrospray-ionization mass spectrometry (ESI-MS)**. The reaction of HU + Mn(III)TTEG-2-PyP^{5+} was also followed by a Bruker micrOTOFQ mass spectrometer equipped with a quadrupole and time-of-flight (Q-TOF) analyzer in positive ion mode. The sample solution was introduced directly into the ESI source via a gas-tight syringe and a syringe pump which was synchronized with the software of the MS instrument. This feature enabled the precise determination of the aging time of the reaction mixture at the instance of data recording, thus time resolved ESI-MS spectra could be collected.

The products of the above mentioned reactions were analyzed by **ion-chromatography (IC)** as well. The ions CN^- and SCN^- were measured using integrated amperometry detection, and OCN^-, SO_3^{2-} and SO_4^{2-} were measured using conductivity detection on a Dionex ICS-3000 instrument with an Ionpac AS16 column.

Typically, the experimental kinetic data were evaluated either by the initial rate method, or by fitting the experimental kinetic curves to the appropriate integrated rate law. Micromath Scientist 2.0 software was used for Levenberg-Marquard least-squares fitting procedures. Multiple sets of representative kinetic curves recorded in a given reaction system, but under different initial conditions were **globally evaluated and fitted** to the constructed kinetic model with the program package ZiTa using the GEAR algorithm.

III) SCIENTIFIC ACHIEVEMENTS

1) Rate and mechanism of water exchange of MnTEt-2-PyP^{5+}, MnTnHex-2-PyP^{5+}, MnTTEG-2-PyP^{5+} and MnTSPP^{3-} at neutral pH.

1.1) With temperature-dependent ^{17}O NMR measurements and adequate data treatment, we found that the axially coordinated water molecules in the cationic MnTEt-2-PyP^{5+}, MnTnHex-2-PyP^{5+} and MnTTEG-2-PyP^{5+} complexes are less labile than in the anionic MnTSPP^{3-} at neutral pH. The lower water exchange rate constants (k_{ex}) for the positively charged complexes are due to a significant decrease in the activation entropy ($\Delta S^{\ddagger}$) from +79 J/mol/K for Mn(III)TSPP^{3-} to ca. 0 J/mol/K for the cationic complexes (cf. Table 1). The large positive value of the activation entropy suggests a limiting dissociative (D) water-exchange mechanism for the Mn(III)TSPP^{3-}, whereas the close to zero entropy values for the cationic complexes are indicative of the interchange (I) mechanism which are proposed to be dissociative interchange (I_d) after further discussion.

1.2) We found that similarly to Fe(III) porphyrins, the crucial factors that determine the water exchange rates are the electron density of the metal center and the steric compression of the complex. The dissociatively activated water exchange is faster when the electron density on the metal center is increased as in the case of Mn(III)TSPP^{3-} where the 4-sulfonatophenyl substituents are strong electron donors, and when the peripheral substituents of the porphyrin are bulky, sterically hindering the complex and extruding water molecules from the inner coordination sphere as in the case of MnTnHex-2-PyP^{5+}.

1.3) The suggested inner sphere electron transfer mechanism for the reactions of the positively charged Mn(III) porphyrins with various biologically important free radicals is further confirmed by the present study. Applying the Fouss equation to the published rate constants of the above redox reactions, we found that the theoretically calculated

rate of substitution of an axial water molecule of a +5 charged complex with a -1 charged ligand is in the same magnitude as the measured rate of dissociative interchange of water molecules. This indicates that the inner sphere coordination of the redox partner is rate limiting before electron transfer can take place.

Table 1. Rate constants and activation parameters of water exchange of selected Mn(III) porphyrin complexes at neutral pH.

	k_{ex}^{298K} (s^{-1})	$\Delta H^{\ddagger}$ (kJ/mol)	$\Delta S^{\ddagger}$ (J/mol/K)	Mechanism
MnTEt-2-PyP^{5+}	4.12×10^6	36 ± 3	4 ± 10	I_d
MnTnHex-2-PyP^{5+}	5.73×10^6	34 ± 7	-2 ± 23	I_d
MnTTEG-2-PyP^{5+}	4.88×10^6	31 ± 5	-13 ± 20	I_d
$MnTPPS^{3-}$	2.74×10^7	54 ± 5	79 ± 19	D

2) Detailed kinetics and mechanism of the reaction of N-hydroxyurea (HU) with MnTTEG-2-PyP^{5+} at basic pH.

1.1) We proved that the catalytic autoxidation of HU to NO_2^- takes place in the HU + Mn(III)TTEG-2-PyP^{5+} reaction system at basic pH under aerobic conditions. The Mn(III)TTEG-2-PyP^{5+}, HU and O_2 dependence of the reaction has been extensively studied and we found that Mn(III)TTEG-2-PyP^{5+} acts as a catalyst and is intact at the end of the process. An adduct formation between Mn(III)TTEG-2-PyP^{5+} and HU (Mn(III)TTEG–HU) is proposed to be the first step of the mechanism, and some of the subsequent steps include O_2 as a reaction partner. The major intermediate is the nitric oxide complex {MnNO} of Mn(II)TTEG-2-PyP^{4+} (Mn(II)TTEG–NO) which is formed either by the direct autoxidation of Mn(III)TTEG–HU or by the reaction between Mn(II)TTEG-2-PyP^{4+} and NO following a ligand-to-metal electron transfer in Mn(III)TTEG–HU to yield Mn(II)TTEG-2-PyP^{4+}

and N-hydroxyurea radical ($HU^{\bullet}$), subsequently NO. The presence of Mn(II)TTEG-2-PyP^{4+} and Mn(III)TTEG–HU was verified in the reaction system by ESI-MS. The thermodynamic stability of Mn(II)TTEG–NO is high, but it undergoes slow autoxidation after its formation. The autoxidation of both Mn(II)TTEG-2-PyP^{4+} and Mn(II)TTEG-NO replenishes Mn(III)TTEG-2-PyP^{5+}. NO and HNO are produced as minor intermediates in the oxidation of $HU^{\bullet}$, and will eventually be oxidized to NO_2^- of relative stability. The detailed mechanism can be seen in Scheme 2. The complete experimental kinetic data set recorded under different initial conditions has been fitted to the kinetic model of Scheme 2 with the previously known rate constants held fix. The results are acceptable (cf. Figure 1).

2.2) We conclude that HU reacts with Mn(III)TTEG-2-Pyp^{5+} like a typical NO donor compound under oxidative conditions, i.e. giving the {MnNO} complex of the cationic Mn(II) porphyrin after directly coordinating to the Mn(III) center (Martí, M. A.; Bari, S. E.; Estrin, D. A.; Doctorovich, F. *J. Am. Chem. Soc.*, 2005, *127*, 4680.). Thus, the reaction of Mn(III)TTEG-2-Pyp^{5+} and HU can be regarded as a model reaction for the catalytic autoxidations of biologically active small molecular NO donors.

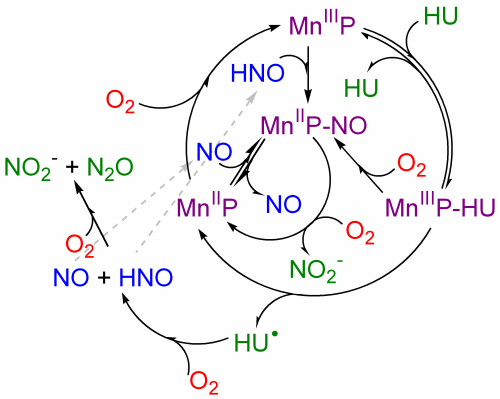

Scheme 2. Proposed kinetic model for the reaction of Mn(III)TTEG-2-Pyp^{5+} with HU under aerobic conditions at basic pH.

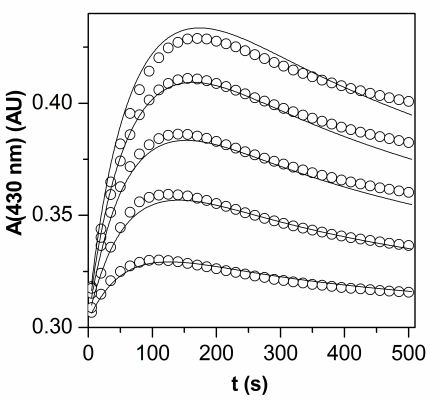

Figure 1. Representative experimental kinetic curves of the reaction of Mn(III)TTEG-2-PyP^{5+} and HU (circles) and the corresponding fit (lines) using the kinetic model from Scheme 2.

3) Detailed kinetics and mechanism of the oxidation of SCN^- by peroxomonosulfate ion (HSO_5^-) at neutral and basic pH.

3.1) We showed that HSO_5^- oxidizes SCN^- to hypothiocyanite ion ($OSCN^-$) at neutral and basic pH. The oxidation of $OSCN^-$ by HSO_5^- also takes place in the reaction system of HSO_5^- + SCN^-. We derived a simple kinetic model, as seen in Scheme 3, valid at neutral and basic pH, and showed that the inclusion of the thermodynamically hardly feasible equilibrium step between SCN^- + HSO_5^- and $OSCN^-$ + SO_4^{2-} presented in the Smith and Wilson kinetic model (Smith, R. H.; Wilson, I. R. *Aust. J. Chem.*, 1967, *20*, 1353-1366.) is not necessary under these conditions. Interestingly the kinetic behavior the reaction system is similar to that of an equilibrium.

3.2) The activation parameters and rate constants of the HSO_5^-/SO_5^{2-} + SCN^- and HSO_5^-/SO_5^{2-} + $OSCN^-$ reactions were determined (Table 2). By critically evaluating the obtained activation parameters we conclude that the rate determining steps in the above oxidation processes are more likely to be two-electron transfer than one-electron transfer steps. Because the rate constant of the oxidation of $OSCN^-$ is

an order of magnitude higher than that of SCN^-, these two compounds compete for the oxidant HSO_5^-/SO_5^{2-}, and the stoichiometric production of $OSCN^-$ is possible only by minimizing the relative rate of the "overoxidation" reaction, using at least a 100-fold excess of SCN^- over HSO_5^-/SO_5^{2-}.

3.3) Our presented methodology gave quantitative information on the kinetics of the oxidation of the antimicrobial $OSCN^-$ by a peroxo compound, which seems to have no precedent in the literature. If the relative reactivities of SCN^- and $OSCN^-$ are expected to be similar towards HSO_5^- and H_2O_2, it is reasonable to assume that the *in vivo* accumulation of $OSCN^-$ during the defensive peroxidase catalyzed $SCN^- + H_2O_2$ reaction is limited by the presence of H_2O_2 itself.

3.4) We found that Mn(III)TMe-4-Pyp^{5+} catalyzes the oxidation of SCN^- by HSO_5^-. The stable product of the oxidation of Mn(III)TMe-4-Pyp^{5+} by HSO_5^- is OMn(IV)TMe-4-Pyp^{4+}, which shows only slight reactivity towards SCN^-, thus cannot be responsible for the observed catalytic effect. We propose that OMn(V)TMe-4-Pyp^{5+} is an intermediate in the Mn(III)TMe-4-Pyp^{5+} + HSO_5^- reaction which can rapidly oxidize SCN^- in the $SCN^- + HSO_5^-$ + catalyst reaction system and be reduced to Mn(III)TMe-4-Pyp^{5+}.

Scheme 3. Kinetic model for the oxidation of SCN^- by HSO_5^-/SO_5^{2-} at neutral and basic pH. The reaction steps marked with italic are fast.

$HSO_5^- + SCN^- \rightarrow SO_4^{2-} + OSCN^- + H^+$	k_1^H	(R1^H)
$HSO_5^- + OSCN^- \rightarrow SO_4^{2-} + O_2SCN^- + H^+$	k_2^H	(R2^H)
$SO_5^{2-} + SCN^- \rightarrow SO_4^{2-} + OSCN^-$	k_1	(R1)
$SO_5^{2-} + OSCN^- \rightarrow SO_4^{2-} + O_2SCN^-$	k_2	(R2)
$2\ O_2SCN^- \rightarrow O_3SCN^- + OSCN^-$		*(R3)*
$O_2SCN^- + OSCN^- \rightarrow O_3SCN^- + SCN^-$		*(R4)*
$O_3SCN^- + 2\ OH^- \rightarrow SO_4^{2-} + CN^- + H_2O$		*(R5)*
$O_3SCN^- + 2\ OH^- \rightarrow SO_3^{2-} + OCN^- + H_2O$		*(R6)*

Table 2. Rate constants and activation parameters of the elementary reactions of $SCN^-/OSCN^-$ + HSO_5^-/SO_5^{2-} as seen in Scheme 3.

Reaction	Studied at pH	k^{298K} ($M^{-1}\,s^{-1}$)	$\Delta H^{\ddagger}$ (kJ/mol)	$\Delta S^{\ddagger}$ (J/mol/K)
R1	13.5	$(1.0 \pm 0.2)\times10^1$	35.2 ± 0.5	-108 ± 2
R2	13.5	$(1.6 \pm 0.1)\times10^2$		
$R1^H$	6.9	$(2.0 \pm 0.2)\times10^2$	26 ± 1	-112 ± 3
$R2^H$	6.9	$(3.3 \pm 0.1)\times10^3$	30 ± 2	-77 ± 5

4) Kinetics and mechanism of the hydrolytic decomposition of thiocyanogen ($(SCN)_2$) and the antimicrobial hypothiocyanite ($OSCN^-$) at slightly acidic and neutral pH.

4.1) Based on our kinetic results, we deduced the rate law for the hydrolytic decomposition of $OSCN^-$ at neutral and slightly acidic pH. According to the analogous hydrolysis chemistry of hypohalites a kinetic model (Scheme 4) has been constructed, which reproduces the measured rate law under limiting conditions. The eventual stable products of the decomposition of $OSCN^-$ at neutral pH are simple inorganic anions: OCN^-, SCN^-, SO_3^{2-} and SO_4^{2-}.

4.2) We found that $(SCN)_2$ decomposes with a similar mechanism (not shown) to that of $OSCN^-$, and the hydrolysis of the two species are interconnected. The lifetime of $OSCN^-$ decreases with decreasing pH and with increasing SCN^- concentration because $OSCN^-$ is converted to $(SCN)_2$ faster under these conditions. The presence of $(SCN)_2$ further decreases the concentration of $OSCN^-$ as a consequence of their rapid irreversible reaction with one another, which was studied independently. The formation of NCS(=O)SCN in this reaction is proposed for the first time in this study on the basis of modeling of the kinetics from which the stoichiometry is obtained, and previously published isotope tracer studies which indicate that a similar intermediate should be unsymmetrical to sulfur atoms.

4.3) Evidence is provided that $OSCN^-$ cannot coexist with $(SCN)_2$ at physiological pH, and that they are not in dynamic equilibrium with each other. Furthermore, previous mechanistic proposals for the formation of $OSCN^-$ in the lactoperoxidase system that invoke $(SCN)_2$ as an intermediate during the enzymatic oxidation of SCN^- by H_2O_2 cannot be correct, because the product of the hydrolysis of $(SCN)_2$ at neutral pH is not $OSCN^-$. Based on these conclusions, the biochemical role of $(SCN)_2$ is questionable.

Scheme 3. Kinetic model and rate law for the hydrolytic decomposition of $OSCN^-$ at neutral and slightly acidic pH.

$HOSCN \rightleftharpoons OSCN^- + H^+$	K_1 fast equilibrium	(R1)
$HOSCN + SCN^- \rightleftharpoons HO(SCN)_2^-$	k_2 and k_{-2} ($K_2=k_2/k_{-2}$)	(R2)
$HO(SCN)_2^- \rightleftharpoons (SCN)_2 + OH^-$	k_3 and k_{-3} ($K_3=k_3/k_{-3}$)	(R3)
$HO(SCN)_2^- + H^+ \rightleftharpoons (SCN)_2 + H_2O$	k_4 and k_{-4} ($K_4=k_4/k_{-4}$)	(R4)
$(SCN)_2 + SCN^- \rightleftharpoons (SCN)_3^-$	K_5 fast equilibrium	(R5)
$OSCN^- + (SCN)_2 \rightarrow NCS(=O)SCN + SCN^-$	k_6, RDS	(R6)
$NCS(=O)SCN + H_2O \rightarrow O_2SCN^- + SCN^- + 2H^+$		*(R7)*
$O_2SCN^- + HOSCN \rightarrow O_3SCN^- + SCN^- + H^+$		*(R8)*
$O_3SCN^- + H_2O \rightarrow SO_4^{2-} + HCN + H^+$		*(R9)*
$O_3SCN^- + H_2O \rightarrow SO_3^{2-} + OCN^- + 2H^+$		*(R10)*

$$v = \frac{\alpha(1-\alpha)k_2k_6\left(k_3+k_4[H^+]\right)[H^+][SCN^-][HOSCN]_T^{\,2}}{k_{-2}\left(k_{-3}[OH^-]+k_{-4}\right)+(1-\alpha)k_6\left(k_{-2}+k_3+k_4[H^+]\right)[HOSCN]_T}$$

$$\alpha = \frac{[H^+]}{K_1+[H^+]}$$

$$[HOSCN]_T = [HOSCN]+[OSCN^-]$$

IV) POSSIBLE APPLICATIONS OF THE RESULTS

Due to the high biological and clinical relevance of the reactions that occur at the metal site of the studied Mn(III) porphyrins, the determination of water exchange rates may advance our insight into their efficacy and mechanism of action, and in turn can impact their further development for both diagnostic imaging and therapeutic purposes.

The possibility of a synergic therapeutic effect of HU and cationic Mn(III) porphyrins analogous to Mn(III)TTEG-2-Pyp^{5+} is not negligible because of the probable acceleration of the *in vivo* production of NO and its metabolites from HU.

The high rate of the HSO_5^- + SCN^- reaction might make Oxone® an attractive choice for technologies aiming the oxidative removal of SCN^- from metallurgical wastewater, keeping in mind that method optimization is required to completely avoid the formation of the toxic CN^- as a product. The results on the kinetics of the oxidation of $OSCN^-$ by a peroxo compound may contribute to the understanding of the bioinorganic chemistry of this bactericide compound.

The mechanistic models for the hydrolytic decomposition of $OSCN^-$ and $(SCN)_2$ address previous empirical observations, including the facts that the presence of SCN^- and/or $(SCN)_2$ decreases the stability of $OSCN^-$, that radio isotopic labeling provided evidence that under physiological conditions decomposing $OSCN^-$ is not in equilibrium with $(SCN)_2$ and SCN^-, and that the hydrolysis of $(SCN)_2$ near neutral pH does not produce $OSCN^-$. These observations are important in understanding the *in vivo* reactivity of $OSCN^-$.

V) LIST OF PUBLICATIONS

Publications covered in the thesis:

4) Detailed kinetics and mechanism of the oxidation of thiocyanate ion (SCN^-) by peroxomonosulfate ion (HSO_5^-). Formation and subsequent oxidation of hypothiocyanite ion ($OSCN^-$)
J. Kalmár*, G. Lente, I. Fábián
Inorganic Chemistry, **2013**, 52(4), 2150-2156.
IF(2011)=4.60

3) Detailed mechanism of the autoxidation of N-hydroxyurea catalyzed by a superoxide dismutase mimic Mn(III) porphyrin: formation of the nitrosylated Mn(II) porphyrin as an intermediate
J. Kalmár, B. Biri, G. Lente*, I. Bányai, A. Budimir, M. Biruš, I. Batinić-Haberle, I. Fábián
Dalton Transactions, **2012**, 41 (38), 11875-11884.
IF(2011)=3.84

2) Mechanism of decomposition of the human defense factor hypothiocyanite near physiological pH
J. Kalmár, K. L. Woldegiorgis, B. Biri, M. T. Ashby*
Journal of the American Chemical Society, **2011**, 133 (49), 19911-19921. *IF(2011)=9.91*

1) Water exchange rates of water-soluble manganese(III) porphyrins of therapeutical potential
A. Budimir, J. Kalmár*, I. Fábián, G. Lente, I. Bányai, I. Batinić-Haberle, M. Biruš*
Dalton Transactions, **2010**, 39 (18), 4405-4410. *IF(2010)=3.65*

Summa IF=22.00

Other publications:

5) Kinetics of formation of the host–guest complex of a viologen with cucurbit[7]uril
J. Kalmár, S. B. Ellis, M. T. Ashby, R. L. Halterman*
Organic Letters, **2012**, 14 (13), 3248-3251. *IF(2011)=5.86*

4) Collision induced dissociation study of the major components of silymarin
Á. Kuki, B. Biri, L. Nagy, Gy. Deák, J. Kalmár, M. Nagy, M. Zsuga, S. Kéki*
International Journal of Mass Spectrometry, **2012**, 315, 46-54. *IF(2011)=2.55*

3) Energy-dependent collision-induced dissociation study of buprenorphine and its synthetic precursors
B. Biri, J. Kalmár, L. Nagy, A. Sipos, M. Zsuga, S. Kéki*
Rapid Communications in Mass Spectrometry, **2011**, *25* (1), 41-49. *IF(2011)=2.79*

2) Hydrochemical study of the source region of Ier (Ér) stream in Satu Mare (Szatmár) County, Romania
J. Kalmár*, M. Braun, I. Fábián
Studia Universitatis Vasile Goldis, Life Sciences Series, **2010**, *20* (4), 57-65. *IF(2010)=Ø*

1) One-versus two-electron oxidation with peroxomonosulfate ion: Reactions with iron(II), vanadium(IV), halide ions, and photoreaction with cerium(III)
G. Lente*, J. Kalmár, Zs. Baranyai, A. Kun, I. Kék, D. Bajusz, M. Takács, L. Veres, I. Fábián
Inorganic Chemistry, **2009**, 48 (4), 1763-1773. *IF(2009)=4.66*

Summa IF=15.86

International conference attendance:

5) Mechanism of decomposition of hypothiocyanite near physiological pH – A new reactive sulfur species (P)
J. Kalmár, M. T. Ashby
Gordon Research Conference, Inorganic Reaction Mechanisms, march 11-16 / 2011 Galveston, Texas, USA.

4) Hydrochemical study of the region Érmellék (P)
J. Kalmár, M. Braun, I. Fábián
International Conference „Natural and artificial ecosystems in the Somes- Cris- Mures- Tisa river basin”, may 7-8 / 2010, Macea, Romania.

3) Water exchange of the water soluble porphyrin Mn(III)TTEG-2-PyP^{5+} and its reaction with N-hydroxyurea (P)
J. Kalmár, G. Lente, I. Fábián, I. Bányai, E. Farkas, A. Budimir, M. Biruš, I. Batinić-Haberle
Inorganic/Bioinorganic Reaction Mechanism Meeting, jan. 7-10 / 2010, Kloster Banz, Germany.

2) The reaction of Mn(III)TTEG-2-PyP^{5+} with N-hydroxyurea (P)
J. Kalmár, G. Lente, I. Fábián, E. Farkas, A. Budimir, M. Biruš, I. Batinić-Haberle
10^{th} International Symposium on Applied Bioinorganic Chemistry, sept. 25-28 / 2009, Debrecen, Hungary.

1) Reactions of the peroxomonosulfate ion with simple inorganic reducing agents (E+P)
G. Lente, G. Bellér, J. Kalmár, Zs. Baranyai, A. Kun, I. Kék, I. Fábián
Gordon Research Conference, Inorganic Reaction Mechanisms, febr. 18-23 / 2007, Ventura, California, USA.

National conference attendance:

10) A peroxomonoszulfát-ion (HSO_5^-) és a tiocianátion (SCN^-) közti reakció kinetikája (E)
Kalmár J., Molnár O., Lente G., Fábián I.
MTA Reakciókinetikai és Fotokémiai Munkabizottság ülése, 2012. ápr. 26-27., Siófok.

9) A hipotiociános-sav (HOSCN) vizes oldatbeli bomlásának mechanizmusa fiziológiáshoz közeli pH-n (E)
Kalmár J., Biri B., K. L. Woldegiorgis, M. T. Ashby
XVII. Nemzetközi Vegyészkonferencia, 2011. nov. 3-6., Kolozsvár.

8) A hipotiociános-sav (HOSCN) vizes oldatbeli bomlásának mechanizmusa fiziológiáshoz közeli pH-n (E)
Kalmár J., Biri B., K. L. Woldegiorgis, M. T. Ashby
MTA Reakciókinetikai és Fotokémiai Munkabizottság ülése, 2011. okt. 27-28., Gyöngyöstarján.

7) Vízoldható Mn(III)-porfirinek vízcsere-sebessége és reakciója N-hidroxi-karbamiddal (E)
Kalmár J., Lente G., Fábián I., Bányai I., A. Budimir, M. Biruš, I. Batinić-Haberle
XV. Nemzetközi Vegyészkonferencia, 2009. nov. 12-15., Marosvásárhely.

6) Vízoldható Mn(III)-porfirinek vízcsere-sebessége és reakciója N-hidroxi-karbamiddal (E)
Kalmár J., Lente G., Fábián I., Bányai I., A. Budimir, M. Biruš, I. Batinić-Haberle
MTA Reakciókinetikai és Fotokémiai Munkabizottság ülése, 2009. okt. 29-30., Gyöngyöstarján.

5) Egy vízoldható Mn(III)-porfirin reakciója N-hidroxi-karbamiddal (E)
Kalmár J., Lente G., Fábián .
44. Komplexkémiai Kollokvium, 2009. máj. 27-29., Siófok.

4) Az Ér forrásvidékének hidrokémiai vizsgálata (E)
Kalmár J.
XXIX. Országos Tudományos Diákköri Konferencia, 2009. ápr. 6-8., Debrecen.

3) Halogenidionok vizes oldatbeli fotolízise (E)
Kalmár J.
XXVIII. Országos Tudományos Diákköri Konferencia, 2007. ápr. 2-4., Szeged.

2) A peroxo-monoszulfátion reakciói egyszerű szervetlen redukálószerekkel (E)
Lente G., Bellér G., Kalmár J., Baranyai Zs., Kun A., Kék I., Fábián I.
MTA Reakciókinetikai és Fotokémiai Munkabizottság ülése, 2006. nov. 2-3., Gyöngyöstarján.

1) Halogenidionok vizes oldatbeli fotolízise (E)
Kalmár J., Lente G., Fábián I.
MTA Reakciókinetikai és Fotokémiai Munkabizottság ülése, 2005. okt. 20-21., Gyöngyöstarján.

(E: Presentation, P: Poster)